

Thrust and bending moment of rigid piles subjected to moving soil

Wei Dong Guo and H.Y. Qin

Abstract: An experimental apparatus was developed to investigate the behaviour of vertically loaded free-head piles in sand undergoing lateral soil movement (w_f). A large number of tests have been conducted to date. Presented here are 14 typical model pile tests concerning two diameters, two vertical pile loading levels, and varying sliding depths with the movement w_f driven by a triangular loading block. Results are provided for driving force as well as for induced shear force (T), bending moment (M), and deflection (y) along the piles with w_f / normalized sliding depth. The tests enable simple expressions to be proposed, drawn from the theory for a laterally loaded pile. The new expressions well capture the evolution of M , T , and y with soil movement observed in current model tests, and the three to five times difference in maximum bending moment (M_{max}) from the two modes of loading. They further offer a good estimate of M_{max} for eight in situ pile tests and one centrifuge test pile. The study quantifies the sliding resistance offered by a pile for the given w_f profiles, pile location (relative to the boundary), and vertical load. It establishes the linear correlation between the maximum thrust (resistance T) and M_{max} , regardless of the magnitudes of w_f .

Key words: ground improvement, model tests, piles, slopes, soil–structure interaction, theoretical analysis.

Résumé : Un appareil expérimental a été développé dans le but d'examiner le comportement de pieux à tête libre chargés verticalement dans du sable qui se déplace latéralement (w_f). De nombreux essais ont été effectués jusqu'à maintenant. Dans cet article, 14 essais modèles typiques couvrant deux diamètres de pieux, deux niveaux de chargement vertical et des profondeurs de glissement variables, avec le mouvement w_f induit par un bloc de chargement triangulaire, sont présentés. Les résultats informent sur la force motrice, la force de cisaillement induite (T), le moment de torsion (M) et la déflexion (y) le long des pieux avec w_f / profondeur de glissement normalisée. Les essais permettent de proposer des expressions simples avec une emphase sur la théorie pour les pieux chargés latéralement. Les nouvelles expressions représentent l'évolution de M , T et y selon les mouvements du sol observés dans les essais, ainsi que la différence d'un facteur trois à cinq fois entre les moments de torsion maximaux (M_{max}) pour deux modes de chargement. De plus, ces expressions offrent une bonne estimation de M_{max} pour huit essais de pieux in situ et un essai centrifuge. L'étude quantifie la résistance au glissement exercée par un pieu pour des profils donnés de w_f , la position du pieu (par rapport à la frontière) et le chargement vertical. Une corrélation linéaire est établie entre la poussée maximale (résistance T) et M_{max} , et ce peu importe la magnitude de w_f .

Mots-clés : amélioration du sol, essais modèles, pieux, pentes, interaction sol–structure, analyse théorique.

[Traduit par la Rédaction]

Introduction

The study of active piles subjected to combined lateral and vertical loads has attracted significant research effort (Meyerhof et al. 1981, 1983; Anagnostopoulos and Georgiadis 1993; Aubeny et al. 2003; Karthigeyan et al. 2007). However, there is limited information available on the study of (passive) pile response when subjected to lateral soil movement and vertical loading (Knappett and Madabhushi 2009). It is not clear how bending moment is related to maximum sliding force (lateral thrust) developed in a passive pile; in particular, once coupled with vertical loads and various soil movement profiles. The correlation needs to be established to facilitate design and inspection of piles used

to stabilize slopes and to support bridge abutments and foundations of tall buildings. Studies to date have principally been based on centrifuge tests (Stewart et al. 1994; Bransby and Springman 1997; Leung et al. 2000), laboratory model tests (Poulos et al. 1995; Pan et al. 2002; Guo and Ghee 2004), and theoretical and numerical analyses (Ito and Matsui 1975; Viggiani 1981; Poulos 1995; Guo 2003). The results are useful in one way or another. Nevertheless, it is unfortunate that the correlation between the moment and the lateral thrust (i.e., shear force in a pile) in the majority of model pile tests was not provided. The force is indeed required to evaluate maximum bending moment (Poulos 1995) in design piles in the aforementioned situation.

Limit equilibrium solutions have been derived for piles in a two-layered cohesive soil (Viggiani 1981; Chmoulian 2004). They allow the maximum bending moment to be correlated to lateral thrust by stipulating (i) a fixed sliding depth and (ii) a uniform soil movement profile (without axial load on the pile head). The solutions are popularly used for passive piles. Likewise, methods based on the p – y curve are widely adopted in practice. However, recent study shows

Received 4 December 2008. Accepted 30 July 2009. Published on the NRC Research Press Web site at cgj.nrc.ca on 2 February 2010.

W.D. Guo¹ and H.Y. Qin. School of Engineering, Griffith University, Gold Coast Campus, QLD 4222, Australia.

¹Corresponding author (e-mail: w.guo@Griffith.edu.au).

that the p - y method significantly overestimated pile deflection and bending moment; therefore, further research is warranted (Frank and Pouget 2008). The response of in situ slope stabilizing piles has been recorded by several researchers (Esu and D'Elia 1974; Fukuoka 1977; Carrubba et al. 1989; Kalteziotis et al. 1993; Smethurst and Powrie 2007; Frank and Pouget 2008). Among others, elastic solutions (Fukuoka 1977; Cai and Ugai 2003) and elastic-plastic solutions² were developed. The former compares well with measured pile response at the reported stress states. The elastic-plastic solutions can capture well the nonlinear response of passive piles at any soil movement. Nevertheless, the effect of soil movement profiles on the response, coupled with an axial load and in a pre-failure state, has yet to be clarified. This can be examined through model pile tests. Above all, a simple correlation between lateral thrust and maximum bending moment is needed to facilitate practical design.

A small-scale experiment can bring about valuable insight into the pile-soil interaction mechanism. It can clarify and quantify key parameters (Abdoun et al. 2003). To examine the response of passive piles, Guo and Ghee (2004) developed a new experimental apparatus. Extensive tests have been conducted to date on piles in sand. Some results were published previously (Guo and Ghee 2005; Guo et al. 2006). This paper presents 14 typical results from testing under an inverse triangular loading block, which were deduced from test piles of two diameters and subjected to two axial load levels. They are analyzed to

- establish the relationship between maximum bending moment and lateral sliding thrust; and
- simulate the evolution of the moment and the sliding thrust with moving soil.

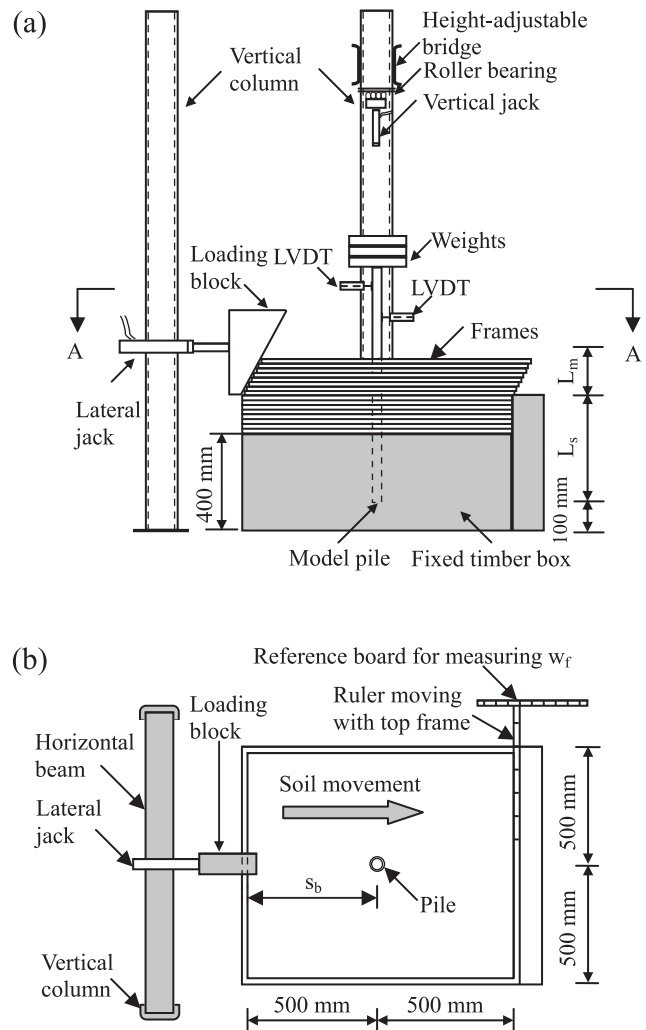
The test results are presented in the form of profiles of bending moment, shear force, and deflection along the pile versus frame movement or normalized sliding depth. The measured correlation between maximum bending moment and lateral thrust and between the thrust and soil movement are provided. These correlations allow newly developed expressions to be validated with respect to the impact of subgrade modulus, vertical load, two different (translational or rotational) loading methods, and effective soil movement. The established correlations are further compared with measured data of eight in situ test piles and one centrifuge test pile.

Apparatus and test procedures

Shear box and loading system

Figure 1 shows an overview of the experimental apparatus developed in the current study. It is mainly made up of a shear box, a loading system, and a data acquisition system. The shear box measures 1 m both in length and width. The upper section of the shear box consists of 25 mm deep square laminar steel frames. The frames, which are allowed to slide, contain the "moving layer of soil" of thickness L_m . The lower section of the shear box comprises a 400 mm height fixed timber box and the desired number of laminar steel frames that are fixed after placement, so that a stable

Fig. 1. Schematic diagram of shear box: (a) elevation view; (b) initial plan view A–A. LVDT, linear variable displacement transducer.

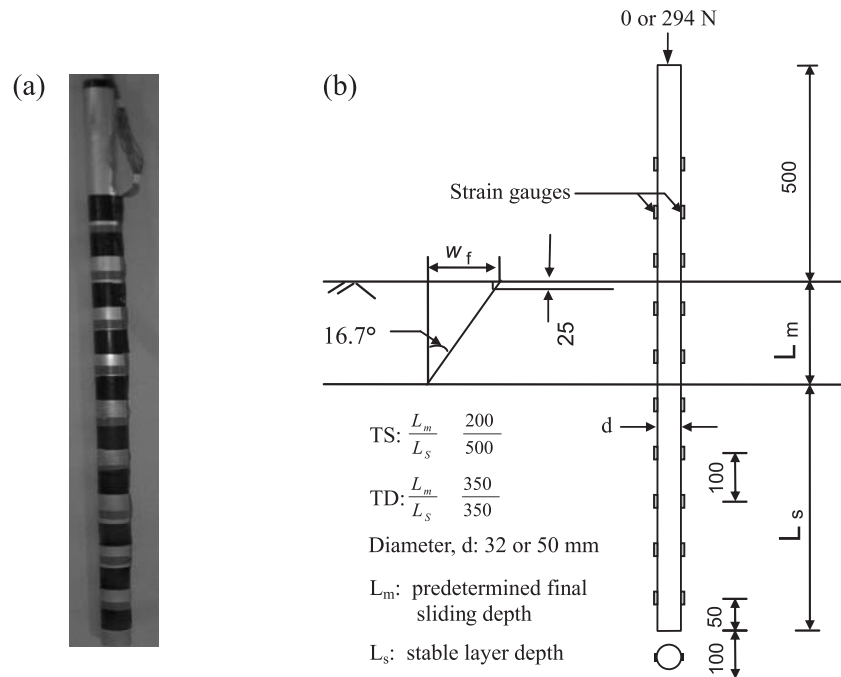


layer of soil of thickness L_s (≥ 400 mm) can be guaranteed. By changing the number of movable frames in the upper section, the thicknesses of the stable and moving layers are varied accordingly. Note that the L_m and L_s are defined at the loading location and that they vary across the shear box. The actual sliding depth L_m around a test pile is unknown, but it would not affect the conclusions being drawn in this paper.

The loading system encompasses a loading block that is placed on the upper movable laminar frames and some weights on top of the test pile. The loading block is made of different shapes to generate various soil movement profiles. The triangular loading block employed here has a (loading) angle of 16.7° (see Fig. 2). A translational frame movement of w_f will induce an increasing sliding depth of $3.33w_f$ (at the loading location) until a pre-specified final depth of L_m . Thereafter, additional frame movement will be uniform over the depth L_m , resulting in an overall trapezoi-

²Guo, W.D. Nonlinear response of slope stabilising piles (unpublished).

Fig. 2. Schematic test of a pile subjected to triangular loading block: (a) instrumented model pile; (b) schematic diagram of testing. d , outer diameter; TD and TS, test designations (refer to text). All dimensions in millimetres.



dal soil movement profile. A hydraulic jack is used to drive the loading block. The jack stroke permits a lateral frame movement w_f of up to 150 mm. Response of the pile is monitored via strain gauges distributed along the piles (see Fig. 2a) and via two linear variable displacement transducers (LVDTs) above the model ground (Fig. 1). The test readings are recorded and processed via a data acquisition system and a computer, which are transferred into “measured” pile response using a purposely designed program discussed later.

Sample preparation and sand properties

Medium oven-dried quartz sand was utilized in this study. Figure 3 shows its particle-size distribution, which has an effective grain size $D_{10} = 0.12$ mm, a uniformity coefficient $C_u = 2.92$, and a coefficient of curvature $C_c = 1.15$. The sand was rained into the shear box through a rainer hanging over the box. The falling height, chosen as 600 mm in this study, was selected to generate a uniform and desired density. This is intended to offer a relative density of 89% and a unit weight of 16.27 kN/m^3 (see Fig. 4). The angle of internal friction of the sand is 38° as evaluated from direct shear tests.

Model pile

The aluminium pipe piles tested each had a length of 1200 mm (see Fig. 2a). They were made of two configurations: one had an outer diameter (d) of 32 mm, a wall thickness (t) of 1.5 mm, and a flexural stiffness ($E_p I_p$) of $1.17 \text{ kN}\cdot\text{m}^2$; the other had $d = 50$ mm, $t = 2$ mm, and $E_p I_p = 6.09 \text{ kN}\cdot\text{m}^2$. Ten levels of strain gauges, placed on the pile surface at intervals of 100 mm, were calibrated prior to the tests. This was done by applying a transverse load in the middle of the pile clamped at both ends. Each gauge

reading measured under various loads was then compared with the theoretically calculated strain. A calibration factor was thus obtained for each gauge, which permits the gauge readings to be converted to actual strains. During the pile test, the strain gauges were protected from damage by covering them with 1 mm of epoxy and wrapping them with tapes.

Test programme

A series of tests were conducted using the triangular loading block. Fourteen typical tests are presented here and summarized in Table 1. Each test is denoted by two letters and two numbers, e.g., TS32-0 and TD32-294: (i) the triangular loading block is signified as “T”; (ii) the “S” and “D” refer to a pre-selected sliding depth (L_m) of 200 and 350 mm, respectively; (iii) the “32” indicates 32 mm in diameter, and (iv) the “0” or “294” represents without or with an axial load of 294 N, respectively. Three types of tests — “pile location”, “standard”, and “varying sliding depth” — are reported here:

- Pile location tests were carried out to investigate the impact of relative distance between the loading block and pile location, etc.
- Standard tests were performed to determine the response to the two final pre-selected sliding depths of 200 and 350 mm.
- Varying sliding depth tests were done to highlight bending moment increases owing to additional movement beyond the triangular profile.

First, for each test, the sample model ground was prepared in the way described previously to a depth of 800 mm. Second, the instrumented pile was jacked in continuously to a depth of 700 mm below the surface, while the (driving) resistance was monitored. Third, an axial load

Fig. 3. Particle-size distribution of sand used.

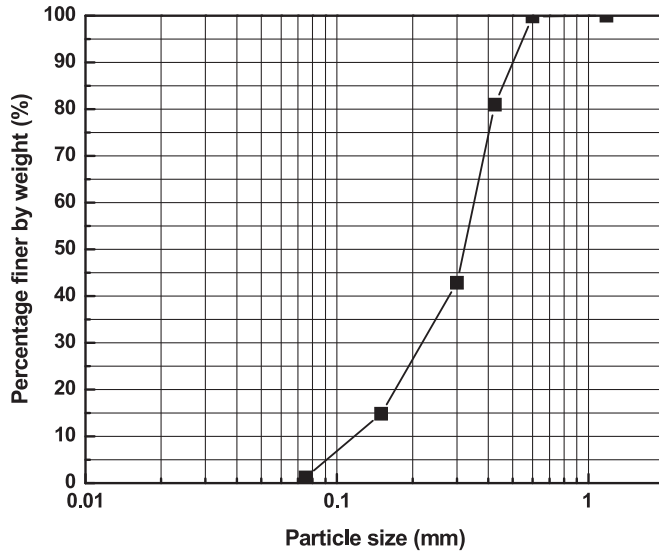
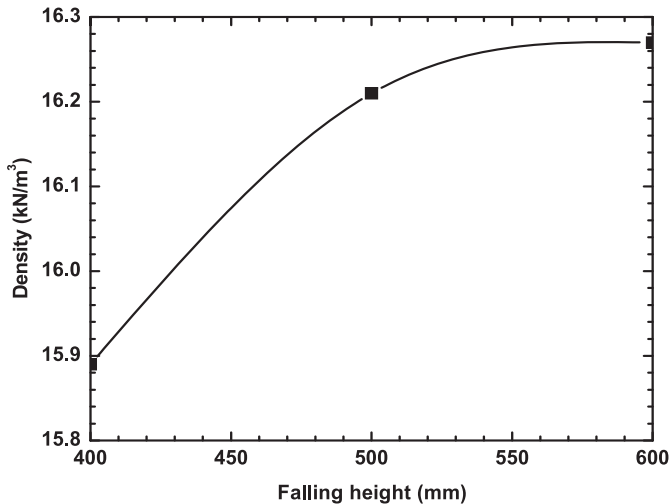


Fig. 4. Relationship between falling height and sand density.



was applied on the pile head using a number of weights (to simulate a free-head pile condition) that were secured (by using a sling) at 500 mm above the soil surface. Fourth, the lateral force was applied via the triangular block on the movable frames to enforce translational soil movement towards the pile. And finally, the sand was emptied from the shear box after each test.

During the passive loading, the gauge readings, the linear variable displacement transducer (LVDT) readings, and the lateral force on the frames were generally taken at every 10 mm movement of the top laminar steel frame (e.g., frame movement, w_f) to ~ 150 mm. A number of trial tests prove the repeatability and consistency of test results presented here.

Determining pile response

A spreadsheet program using Microsoft Excel VBA was written to process and analyze the data obtained from strain gauges and LVDTs. The inclination and deflection profiles along the pile were derived, respectively, from first and second order numerical integration of the bending moment pro-

file. The shear force and soil reaction profiles were deduced by using single and double numerical differentiation of the bending moment profile, respectively. With this program, typical response profiles of bending moment, shear force, soil reaction, deflection, and rotation profiles (Guo and Qin 2006) were deduced for all the tests. They allow the following response to be gained for typical frame movement w_f : maximum bending moment, M_{max} ; depth of the moment, d_{max} ; maximum thrust (shear force in the pile), T_{max} ; and pile deflection at the groundline, y_t (see Table 1).

Influence factors on test results

The current test apparatus allows nonuniform mobilization of soil movement across the shear box. The resulting impact is revealed by the pile location tests. A pile (with $d = 32$ mm) was installed at a distance s_b of 340, 500 or 660 mm from the loading jack side. For instance, a s_b of 500 mm is for a pile installed at the centre of the box. Driving the loading block at the pre-specified final sliding depth of 200 mm, three tests were conducted. The M_{max} obtained is plotted against s_b in Fig. 5. It shows a reduction of ~ 32 kN·mm (at $w_f = 70 \sim 80$ mm) in the moment as the pile was relocated from $s_b = 340$ to 500 mm, and a reduction of ~ 10 kN·mm from $s_b = 500$ to 660 mm. The total maximum moment was $45 \sim 50$ kN·mm for the pile tested at the centre of the box. All the piles reported subsequently were tested at the centre.

Test results

Driving force and lateral force on frames

The jack-in forces for six typical tests were recorded during the installation. They are plotted in Fig. 6. The figure shows a more or less linear increase in driving force with the pile penetration. At the final penetration of 700 mm, the average total forces of the same diameter piles reach 5.4 kN ($d = 50$ mm piles) and 3.8 kN ($d = 32$ mm piles), with a variation of $\sim \pm 20\%$. This reflects the possible variations in model ground properties, as the jack-in procedure was consistent. (Note the axial load of 294 N on the pile head was 7% \sim 9% of the final jacking resistance). The average shaft friction for the installation is estimated as 54 kPa ($d = 32$ mm) and 49.1 kPa ($d = 50$ mm), ignoring the end resistances on the open-ended piles.

Total lateral force on the frames was recorded via the lateral jack during the tests upon each 10 mm frame movement (w_f). They are plotted in Fig. 7 for the six tests. Figures 8a–8g provide the photos taken during the test TS50-294 for a few typical w_f . Figure 7 demonstrates the following:

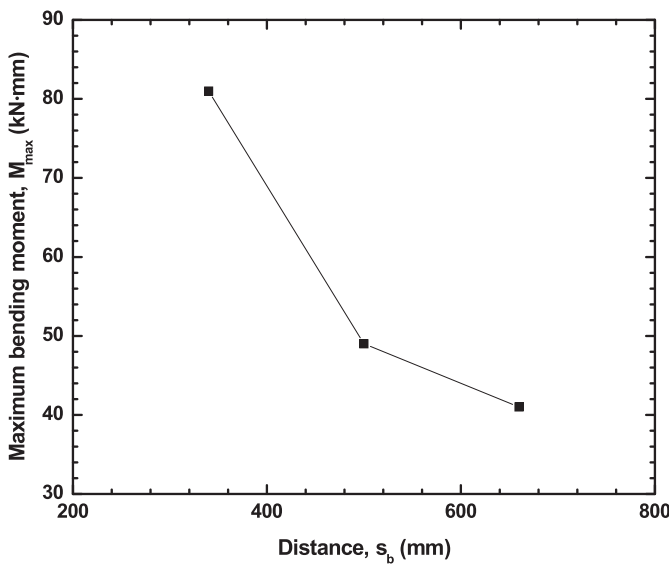
- In general, force linearly increases with the frame movement until it becomes constant.
- Shear modulus of the sand, G_s , is deduced as $15 \sim 21$ kPa using the linear portion of each force–movement curve. For instance, with the TS test series, the maximum shear stress τ is estimated as $4.5 \sim 5.0$ kPa ($= 4.5 \sim 5.0$ kN on loading block over shear area of 1.0 m²). The maximum shear strain γ is evaluated as $0.25 \sim 0.3$ ($= w_f/L_m$, with $w_f = 50 \sim 60$ mm and $L_m = 200$ mm), assuming the shear force is transferred across the sliding depth L_m of 200 mm. The ultimate shear resistance offered by the pile is ~ 0.6 kN (see Fig. 9), which accounts for $\sim 10\%$ the total applied force of $5 \sim 8$ kN on the frames. The de-

Table 1. Summary of 14 typical pile tests.

Test description	Frame movement at ground surface, w_f (mm)	Maximum bending moment, M_{max} (kN·mm)		Depth of M_{max} , d_{max} (mm)	Maximum shear force, T_{max} (N)		Pile deflection at groundline, y_i (mm)	L_m/L_s (mm)
		Tension side	Compression side		Stable layer	Sliding layer		
Pile location								
TS32-0 ($s_b = 340$)	60/80	63.8/81.0	—	400	266.9/327.7	266.6/325.8	11.5/14.8	200/500
TS32-0 ($s_b = 660$)	60/80	30.0/40.0	—	400	114.9/150.3	120.4/153.7	7.8/10.8	200/500
Standard tests ($s_b = 500$)								
TS32-0 ($L_m = 200$)	60/70	39.3/49.7	-34.2/-45.0	370	147.2/183.8	159.8/201.1	7.1/10.3	200/500
TS32-294	60/90	29.8/78.6	-26.8/-76.5	375	108.5/295.5	98.0/279.9	5.4/13.1	200/500
TS50-0	60/80	45.8/89.2	-37.9/-80.2	380	191.9/363.9	180.3/355.7	2.9/7.2	200/500
TS50-294	60/80	58.5/115.6	-59.2/-120.0	400	229.6/445.5	241.4/467.5	3.5/7.3	200/500
TD32-0	120	119.5	-112.1	450	495.9	414.8	58.7	350/350
TD32-294	120	124.6	-117.5	465	532.4	463.5	73.8	350/350
TD50-0	120	93.2	-84.4	450	393.8	353.1	58.9	350/350
TD50-294	120	143	-135.1	450	577.6	453.4	67.5	350/350
Varying sliding depth ($s_b = 500$)								
T32-0 ($L_m = 125$)	40/60	5.2/5.7	—	325	18.9/18.2	22.8/22.5	0.5/0.6	125/575
T32-0 ($L_m = 250$)	80/120	62.6/123.5	—	450	258.1/509.4	233.9/457.3	22.4/47.7	250/450
T32-0 ($L_m = 300$)	100/150	115.3/175.0	—	450	450.6/675.2	399.4/619.6	25.1/54.8	300/400
T32-0 ($L_m = 350$)	120/150	118.1/140.0	—	475	471.7/557.3	406.7/535.3	42.2/73.9	350/350

Note: Except for L_m/L_s , “/” denotes two separate measurements at the two specified values of w_f .

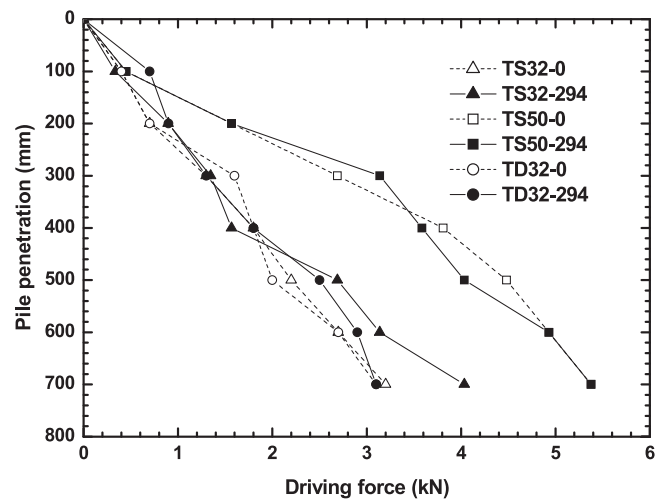
Fig. 5. Variation of maximum bending moment, M_{max} , versus distance of pile from loading side, s_b .



terminated shear stress and modulus may thus be reduced by ~10% for the tests without the pile.

- Average overburden stress, σ_v , at the sliding depth of 200 mm is about 1.63 kPa ($= 16.3 \times 0.1$). At this low stress level, sand dilatancy is evident, which generates a number of “heaves” (see Fig. 8h).
- Lateral force attained a maximum value either around $w_f = 50 \sim 60$ mm (TS series) or around $90 \sim 120$ mm (TD series), and dropped slightly afterwards. The slight fluctuation in the force at large frame movements reflects stress build-up and redistribution around the pile as exhibited by the gradual formation of “heaves”. The pile

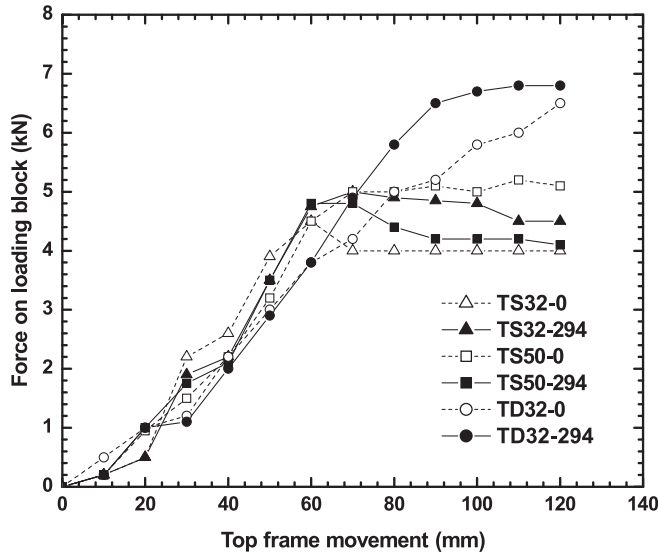
Fig. 6. Jack-in resistance measured during pile installation.



response, however, attained a maximum value at a higher w_f of either 70~90 mm (TS series) or 120 mm (TD series) shown later, indicating a difference of ~30 mm in w_f (i.e., w_i shown later) in transferring the applied force to the pile.

Figure 8 shows the sequential frame movements in lateral and vertical dimensions as the loading block advances. Table 2 shows the typical w_f and the sliding depth induced. A sliding depth ratio R_L is defined as the ratio of thickness of moving soil (L_m) over the pile embedment length (i.e., $L = L_m + L_s$). It is utilized later to quantify the impact of depth of moving layer. For instance, in the TS test series, a $w_f \leq 60$ mm would correspond to a triangular profile to a sliding depth L_m of 200 mm, otherwise to a trapezoidal soil movement profile with a constant $R_L = 0.29$.

Fig. 7. Total applied force on frames against frame movements.



Response of M_{max} , d_{max} , and y_t versus w_i (w_f)

Figure 10 shows the profiles of bending moment, shear force, and pile deflection deduced from the test on the 32 mm diameter pile without axial load (TS32-0). Figure 11 provides the same profiles for the test on the pile with a load of 294 N (TS32-294). They reflect the impact of the triangular movement profile for $w_f \leq 60$ mm and that of the trapezoidal profile afterwards. Critical responses of maximum bending moment, M_{max} , depth, d_{max} , and head deflection at groundline, y_t , are obtained and highlighted below:

- At the maximum response state and without axial load (TS32-0), $M_{max} = 49.7$ kN·mm, $d_{max} = 370$ mm, and $y_t = 10$ mm. The pile mainly rotated (see Fig. 10) about the pile tip.
- Imposing the axial load, the M_{max} increases to 78.6 kN·mm (i.e., 60% increase compared with without load) (see Fig. 11). Negative bending moment was observed around the sand surface at the initial stage with $w_f = \sim 40$ mm ($R_L < 0.17$). The pile rotated about a depth of 550~700 mm (pile tip level) and induced a deflection y_t of ~ 13 mm (i.e., 30% increase).

The strongest response profiles are observed at $w_f = 70 \sim 90$ mm ($d = 32$ mm) for the two tested piles. They are plotted in Figs. 12a and 12b along with those reported previously for $d = 50$ mm (Guo and Qin 2006). The evolution of the maximum bending moment M_{max} and shear force T_{max} are furnished in Figs. 13a and 13b against the movement w_f (for $d = 50$ and 32 mm), respectively. The figures demonstrate the following:

- A small thickness of moving soil (with $R_L < 0.17$, thus $L_m < 120$ mm) did not cause sand to move around the piles located at $s_b = 500$ mm. The initial frame movement w_f (denoted by w_i hereafter) of 37 mm caused trivial response for each of the four test piles. An effective frame movement should be $w_f - w_i$ (mm).
- As the w_f increases from 37 to 80 mm ($R_L = 0.17 \sim 0.29$), the M_{max} for all tests increases proportionally, irrespective of the axial loads; perhaps a triangular soil movement profile prevailed for the w_f . At higher w_f (>80~90 mm),

the M_{max} maintains a constant value and conforms to a trapezoidal soil movement.

- When $w_f = 37 \sim 80$ mm, the M_{max} in tests with the axial load (e.g., TS32-294 and TS50-294) exhibits a “delayed” increase in stiffness and attains a high ultimate value, compared with the pile without the load. (The effect is more pronounced for the deep sliding case, as shown subsequently.) A 60% increase in the M_{max} owing to the axial load for the 32 mm diameter piles is noted compared with 30% for the 50 mm diameter piles.

The w_i captures the impact of the evolution of strain wedges carried by the loading block. For instance, at $w_f = 30$ mm, $L_m = 105$ mm, the lateral extent (at the surface) of the wedge is calculated as 225 mm ($= 105 \tan(45^\circ + 40^\circ/2)$), the frictional angle of 40° is used to account for the compaction effect associated with the moving). This extent is vindicated by the few “heaves” mentioned earlier (see Fig. 8h). The correlation between the maximum shear force T_{max} and M_{max} is discussed later.

Response at deepest sliding depth

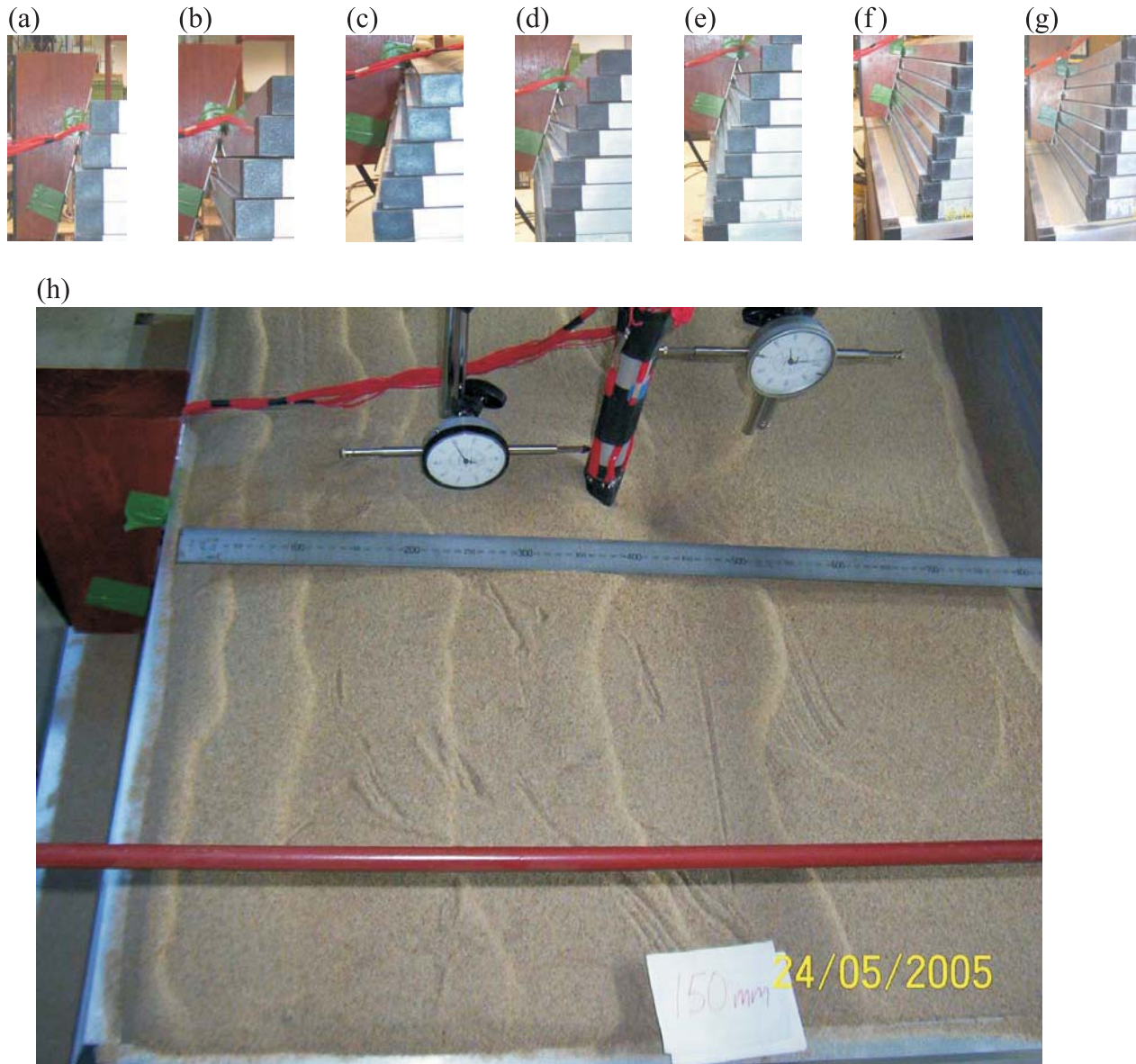
Figures 14 and 15 provide the response profiles obtained using the deepest pre-selected sliding depth of 350 mm and the triangular loading block (TD32-0 and TD32-294). Without the axial load, the 32 mm diameter pile rotated principally about the middle pile embedment and the y_t reached 46 mm at $w_f = 110$ mm. Imposing the axial load of 294 N (TD32-294), the same size pile translated and rotated around the pile tip and the y_t reached 62.5 mm. The moment and shear force profiles for the 32 mm piles at the maximum state ($w_f = 120$ mm) are depicted in Figs. 16a and 16b, respectively, together with those for $d = 50$ mm. The evolution of the maximum bending moments and shear forces with the advance of the frames is illustrated in Figs. 17a and 17b. These figures show the following features:

- The reaction from the 50 mm piles is negligible within a w_i of 30 mm, which is less than 37 mm for $d = 32$ mm piles.
- The axial load causes constant bending moments down to a depth of 200 mm (Fig. 16), below which the moment distribution resembles the one from TS tests (Fig. 12) and it causes the M_{max} increase to ~ 143 kN·mm (see Fig. 16) that occurs at a depth d_{max} of 0.465 m.
- The thrust T_{max} and the M_{max} in the pile will in general attain higher values than those seen in Figs. 14–17, as the movement w_f of 120 mm just mobilizes a sliding depth L_m of 350 mm (see Table 2).

Effect of progressive moving sand on M_{max}

The evolution of M_{max} with the normalized sliding depth R_L is given in Fig. 18a. It shows three distinct stages: (i) a small value of M_{max} at $0 \leq w_f < 37$ mm ($R_L < 0.17$); (ii) the linear increase in M_{max} owing to the triangular movement profile with $37 \leq w_f < 60$ mm ($L_m = 200$ mm, $R_L = 0.29$) or with $37 \leq w_f < 120$ mm ($L_m = 350$ mm, $R_L = 0.5$); and (iii) the moment increases at either $R_L = 0.29$ or 0.5 that are caused by uniform movement beyond the triangular movement. The moment increases were determined by conducting four more tests on the piles ($d = 32$ mm) to the pre-selected final sliding depths of 125, 250, 300, and 350 mm ($R_L =$

Fig. 8. Progressively moving sand induced by a triangular loading block: $w_f =$ (a) 10 mm; (b) 20 mm; (c) 30 mm; (d) 50 mm; (e) 70 mm; (f) 110 mm; (g) 140 mm. (h) Overview of sand heaves at $w_f = 150$ mm.



0.179, 0.357, 0.429, and 0.5, respectively) without axial load. The magnitudes of M_{\max} obtained were 5.2, 62.6, 115.3, and 118.1 kN-mm upon initiating the trapezoidal profile (see Table 2). They finally reached 5.7, 123.5, 175.0, and 140.0 (not yet to limit) kN-mm, respectively. These values are plotted against R_L , together with the TS32-0 test, in Fig. 18b. The M_{\max} along with d_{\max} , T_{\max} , and y_t are provided in Table 1. Note that M_{\max} and T_{\max} from T32-0 ($L_m = 350$ mm) at $w_f = 120$ mm are 1.2% and ~5% less than those from TD32-0, showing the repeatability and accuracy of the current tests.

Simple solutions

Relationship between M_{\max} and T_{\max}

Guo demonstrated that analytical solutions for laterally

loaded (active) piles can be employed to study passive piles subjected to soil movement, for which the lateral load P is taken as the maximum sliding force, T_{\max} , induced in a pile.^{2,3} This use with particular reference to rigid piles is further corroborated using the measured correlation between M_{\max} and T_{\max} and between the effective $y_o (= w_f - w_i)$ and T_{\max} .

Solutions for active rigid piles

Given a free-head, floating-base, laterally-loaded pile, elastic solutions offer (Scott 1981)

$$[1] \quad \begin{aligned} M_{\max} &= (0.148 \sim 0.26)PL \\ d_{\max} &= (0.33 \sim 0.42)L \end{aligned}$$

where P is the lateral load applied at the pile head level and

³Guo, W.D. A pragmatic approach for rigid passive piles in sand. Submitted for publication.

Fig. 9. Variation of maximum shear force versus lateral force on loading block.

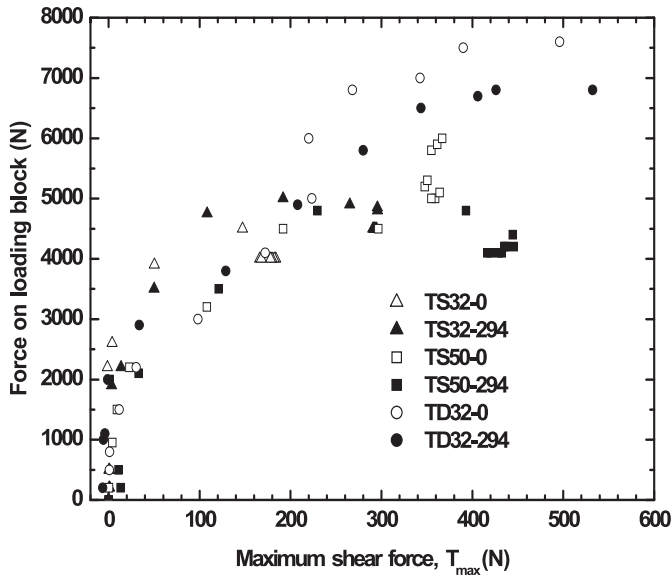


Table 2. Frame movement (w_f) versus depth of moving soil (L_m).

Frame movement, w_f (mm)	Number of fully mobilized frames	Depth of soil movement, L_m (mm)	Sliding depth ratio, R_L
Triangular profile (final $L_m = 200$ mm)			
10	2	50	0.07
20	3	75	0.10
30	4	100	0.14
50	6	150	0.21
70	8	200	0.29
110	8	200	0.29
120	8	200	0.29
Triangular profile (final $L_m = 350$ mm)			
60	8	200	0.29
70	9	225	0.32
80	10	250	0.36
90	11	275	0.39
100	12	300	0.43
110	13	325	0.46
120	14	350	0.50

d_{max} is the depth of maximum bending moment. The coefficient of 0.33 or 0.148 is used for a uniform k , whereas 0.42 or 0.26 is for a Gibson k (Scott 1981). For the pile, elastic-plastic solutions provide the following correlation (Guo 2008):

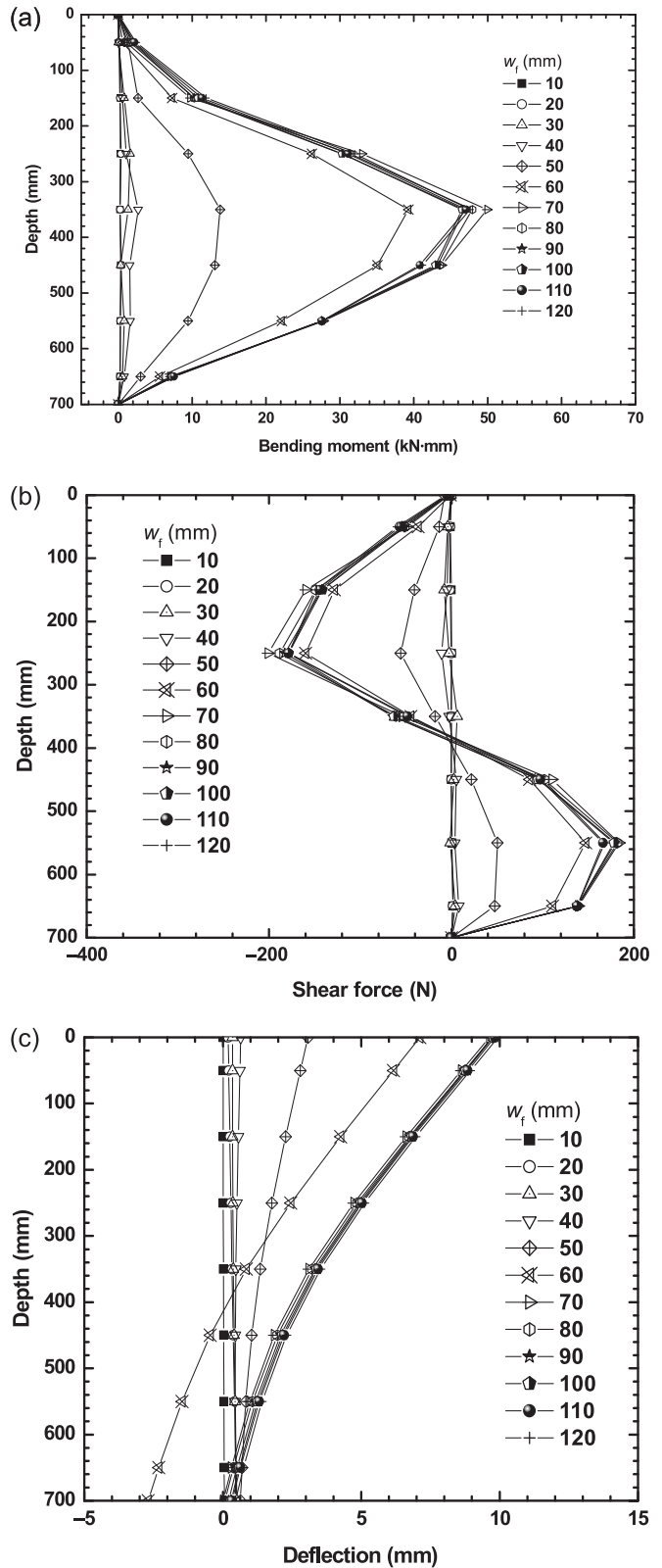
$$[2] \quad M_{max} = \left(\frac{2}{3}d_{max} + e\right)P$$

where e is the real or fictitious free-length of the lateral load above the ground surface. Equation [2] is of identical form to that developed for laterally loaded piles at the ultimate state (Broms 1964).

Use of equivalent load for passive piles

Equations [1] and [2] are used for passive piles by replac-

Fig. 10. Response of pile during TS32-0 with respect to (a) bending moment; (b) shear force; (c) deflection.



ing load P with T_{max} . This is justified from the following two new experimental outcomes, in addition to the similarity of on-pile force profiles between passive and active loading

Fig. 11. Response of pile during TS32-294 with respect to (a) bending moment; (b) shear force; (c) deflection.

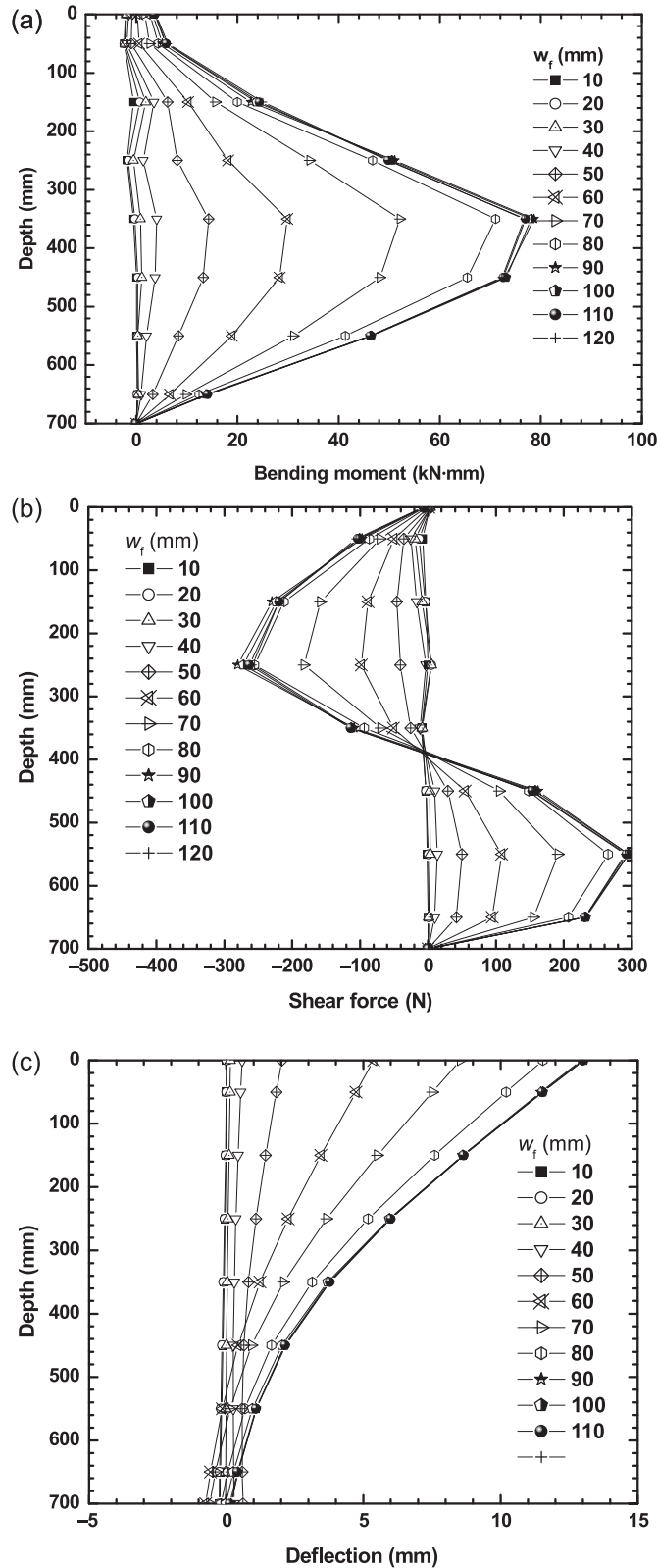
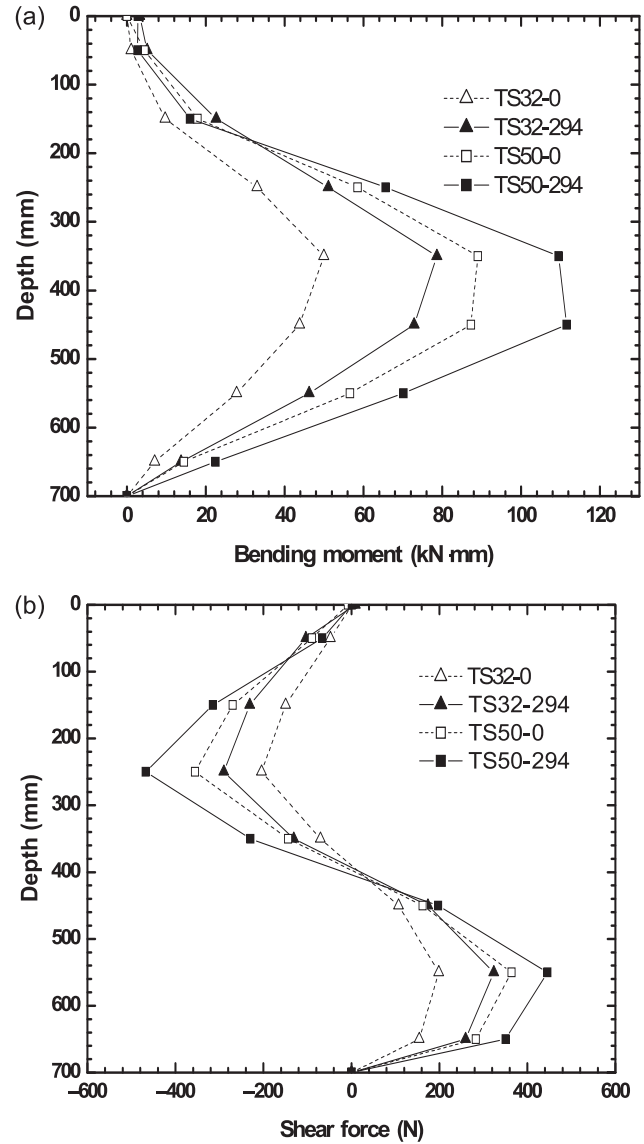


Fig. 12. Maximum response profiles of piles (final sliding depth = 200 mm): (a) bending moment profiles (measured); (b) shear force profiles (measured). Data for TS50-0 and TS50-294 from Guo and Qin (2006).



Figs. 12a and 16a) shows that $d_{max} = 0.35 \sim 0.4$ m or $(0.5 \sim 0.6)L$, such that $M_{max} = (0.33 \sim 0.4)LT_{max}$.

(2) The correlation between T_{max} and M_{max} is observed as linear for all the current model tests, as is demonstrated in Figs. 19a and 19b, and for almost all the w_f . Using $P = T_{max}$ in eq. [2] to fit the measured data in Figs. 19a and 19b allows $M_{max} = 0.357T_{max}L$ to be realized.

Points (1) and (2) indicate an elastic-plastic pile-soil interaction for the current model piles and eq. [1] can be rewritten as

$$[3] \quad M_{max} = (0.148 \sim 0.4)T_{max}L$$

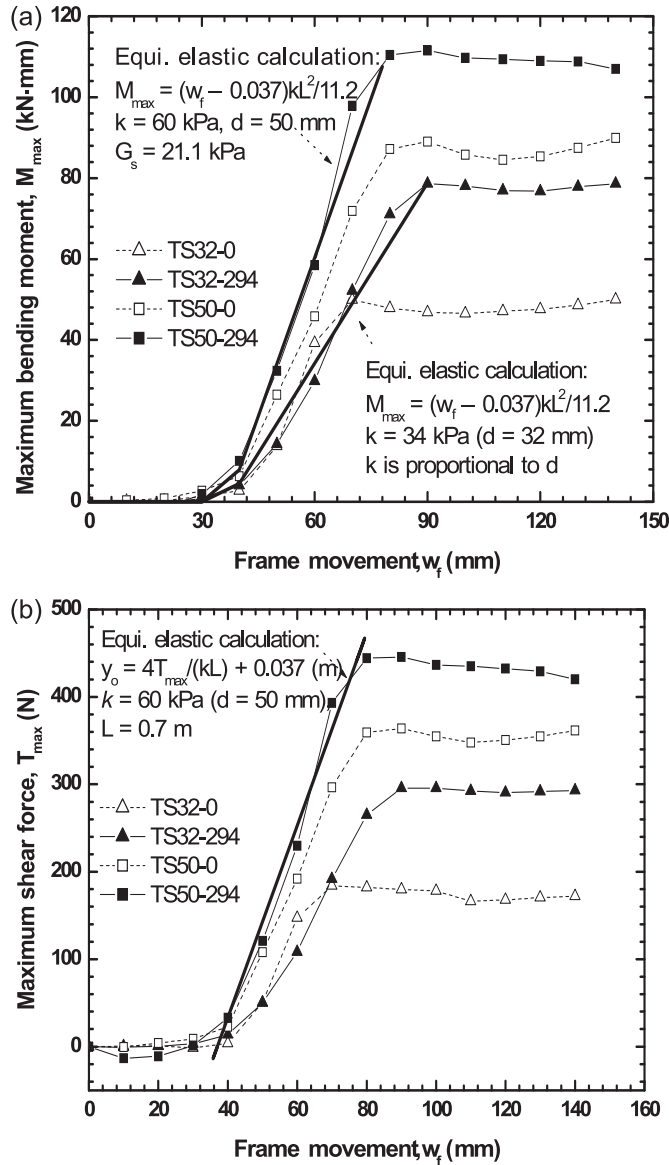
revealed previously (Guo 2003; see footnote 3 (footnote 2 in Web version)):

(1) The bending moment profile for the passive piles (see

Equivalent elastic solutions for passive piles

The current model tests on passive piles support the following hypotheses:

Fig. 13. Evolution of maximum response of piles (final sliding depth = 200 mm): (a) measured M_{max} ; (b) measured T_{max} . Equi., equivalent; k , modulus of subgrade reaction; y_0 , effective frame movement.



- The distance between the pile and the loading block s_b renders a significant portion of the initial frame movement w_i of 30~37 mm to cause a rather small reaction in the pile.
- The effective frame movement of $w_f - w_i (= y_0)$ causes the groundline deflection, y_t , during the passive loading process. Any pile–soil relative rigid movement is incorporated into the w_i and the modulus of subgrade reaction, k . The y_0 may be grossly estimated by using elastic theory for a lateral pile in a homogenous soil

$$[4] \quad y_0 = 4T_{max}/(kL)$$

where $k = (2.4 \sim 3)G_s$ (Guo 2008a). The k here is proportional to pile diameter, d , as is noted in later calculations.

These observations offer

Fig. 14. Response of pile during TD32-0 with respect to (a) bending moment; (b) shear force; (c) deflection.

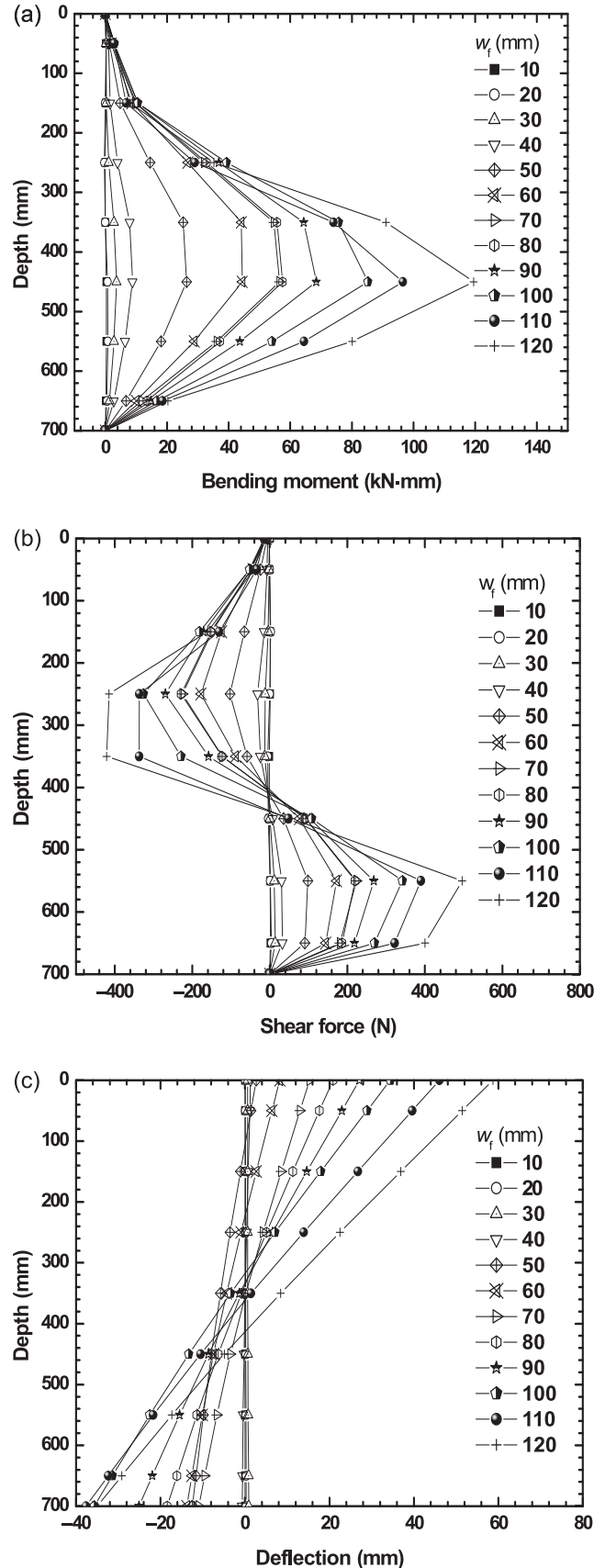


Fig. 15. Response of pile during TD32-294 with respect to (a) bending moment; (b) shear force; (c) deflection.

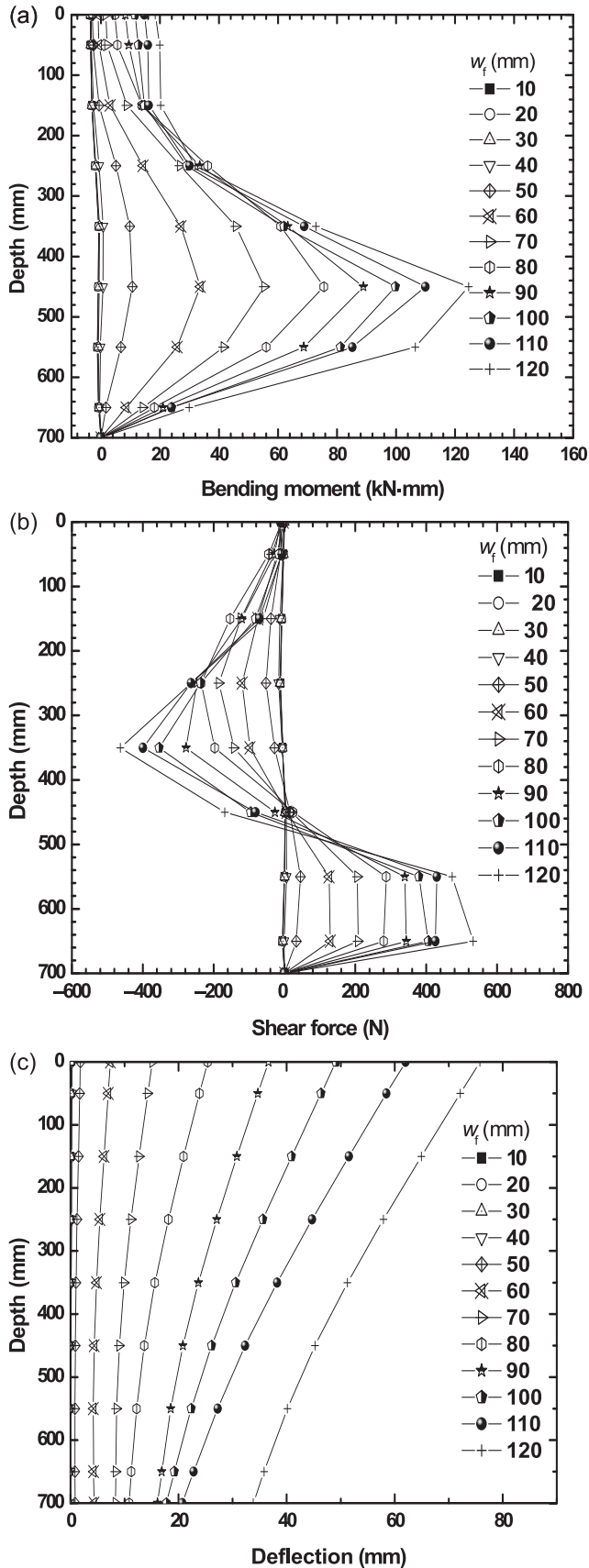
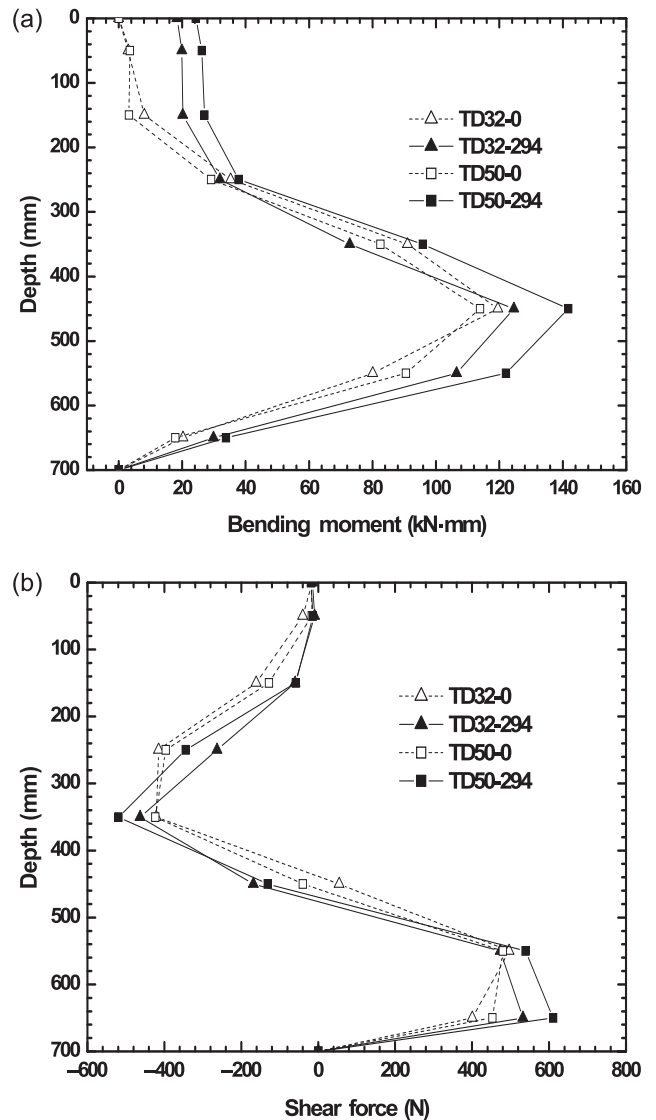


Fig. 16. Maximum response profiles of piles (final sliding depth = 350 mm): (a) bending moment profiles (measured); (b) shear force profiles (measured).



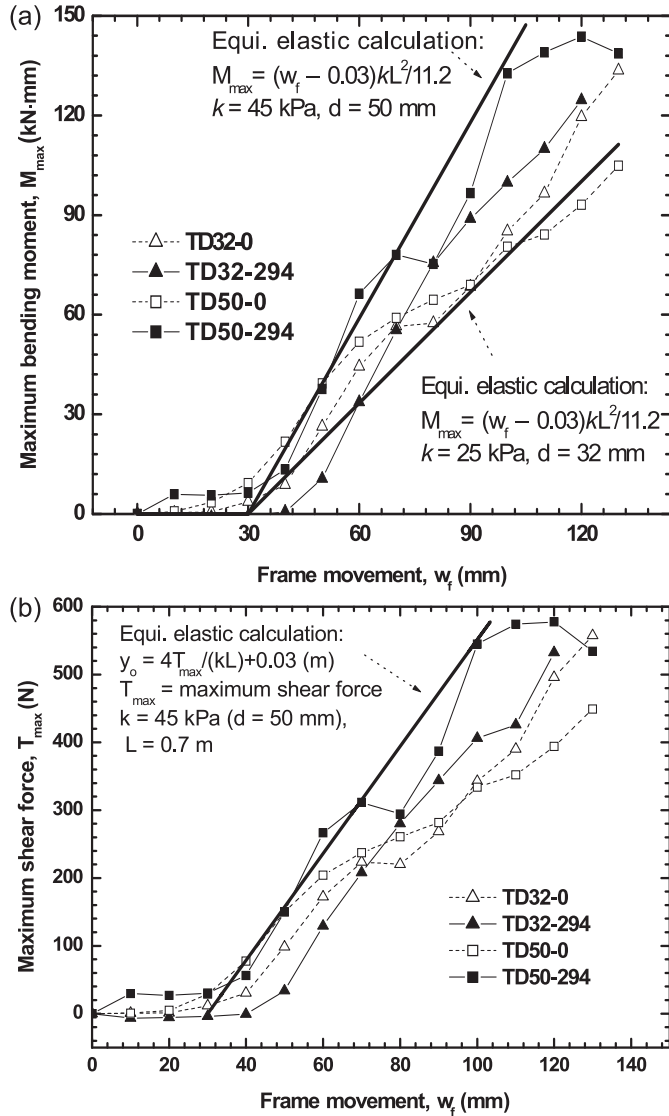
$$[5] \quad T_{\max} = (w_f - w_i)kL/4$$

and eq. [3] may be rewritten as

$$[6] \quad M_{\max} = (w_f - w_i)kL^2/(10 \sim 27)$$

where w_i is the initial frame movement that depends on s_b , the pile diameter, and the loading manner. For instance, $w_i = 0.03 \sim 0.037$ m (the current translational tests) and $w_i = 0.0$ for the rotational tests reported by Poulos et al. (1995). The value of $15.38 \sim 27$ corresponds to the elastic case of the Gibson $k \sim \text{constant } k$, whereas a value of 11.2 or 10 is adopted for the case shown in Fig. 19 and the rotating tests shown in Fig. 18b, respectively. Hereafter in this paper, all “elastic calculation” is based on a value of 15.38 (Gibson k) unless specified otherwise. The length L for each pile was taken as the smallest values of L_i (pile embedment in i th layer, $i = 1, 2$ for sliding and stable layer, respectively, in this paper) and the equivalent length of the rigid pile, L_{ci} . For model tests, as the sliding layer is not evident around a

Fig. 17. Evolution of maximum response of piles (final sliding depth = 350 mm): (a) measured M_{max} ; (b) measured T_{max} .



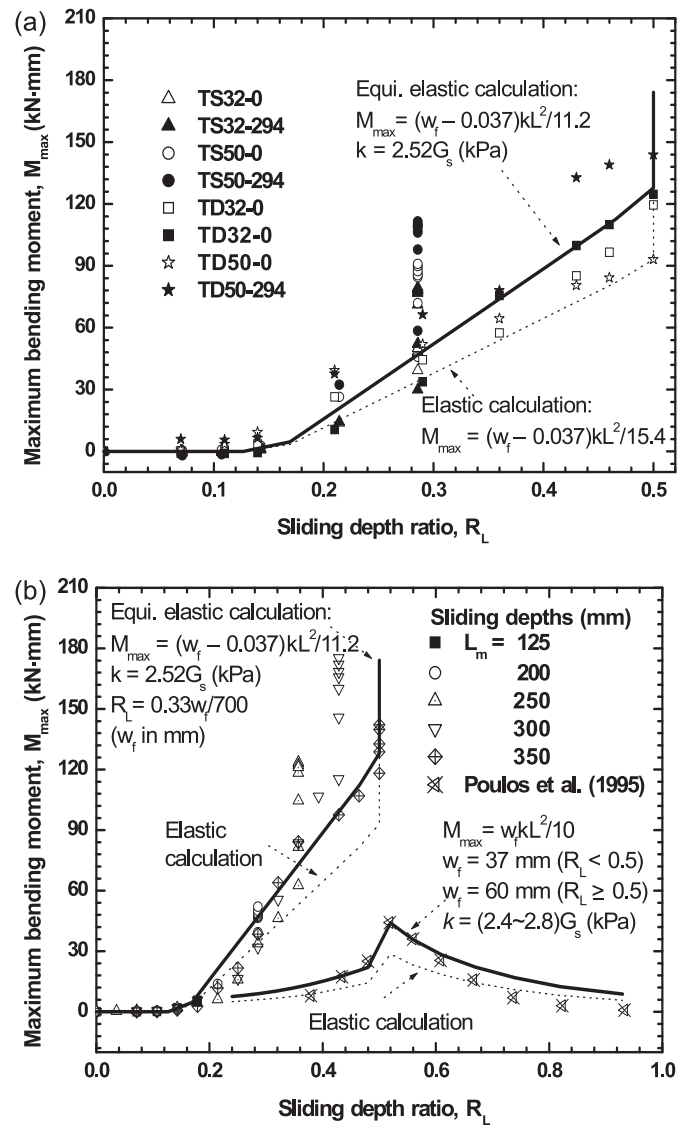
test pile, the length L has to be taken as the pile embedment length. The L_{ci} is given by (Guo and Lee 2001)

$$[7] \quad L_{ci} = 1.05d(E_p/\bar{G}_s)^{0.25}$$

where E_p is the Young's modulus of an equivalent solid cylinder pile and \bar{G}_s is the average shear modulus of soil over the depth of the i th layer. When using these expressions, it must be stressed that

- The modulus k is deduced from the overall sliding process characterized by the sand pile–shear box interaction. This should not be adopted for predicting the pile deflection at groundline, y_t , and for the values provided in Table 1 that reflect a local pile–soil interaction.³ A higher modulus k is generally seen for predicting y_t rather than the k for overall sliding, especially for a local pile–soil interaction (shallow sliding depth). The pile deflection, y_t , in the overall sliding process does encompass a significant component of “rigid” rotation, although in the local interaction it does not. Two local interaction cases are as

Fig. 18. Variation of maximum bending moment versus sliding depth ratio. Measured M_{max} for (a) $L_m = 200$ and 350 mm and (b) various sliding depths.



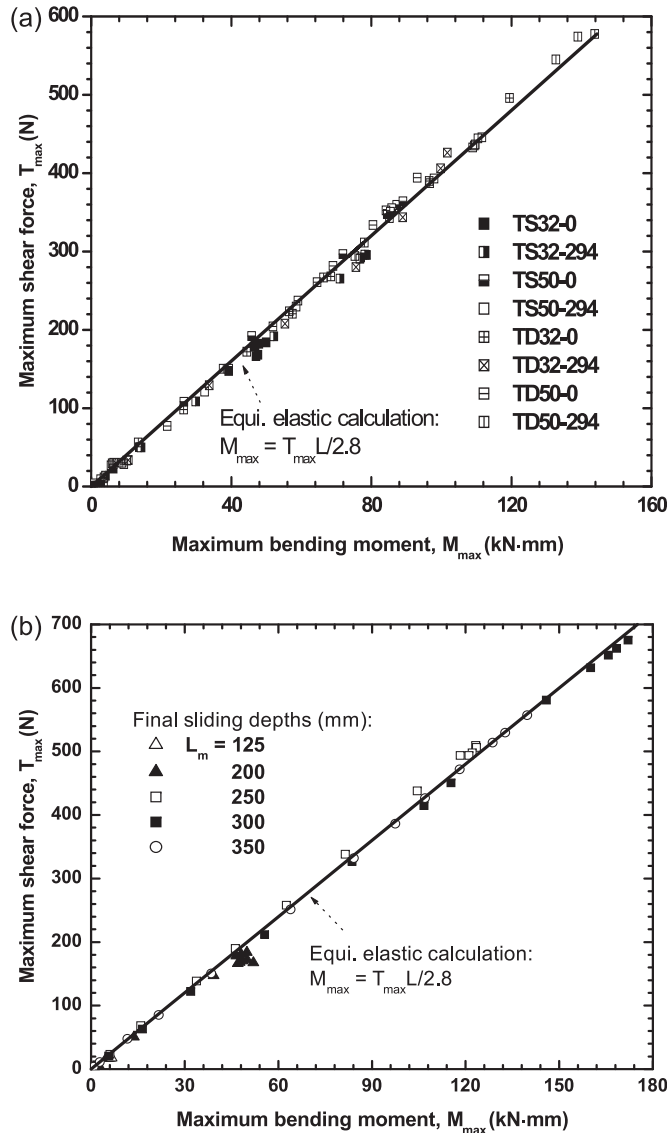
follows. (i) The deflection at groundline y_t was measured as 46 mm for TD32-0 under $w_f = 110$ mm. Given the measured $T_{max} = 0.4$ kN, $k = 50$ kPa, and $L = 0.7$ m, eq. [4] yielded a similar deflection y_o of 45.7 mm. (ii) The y_o at $w_f = 110$ mm was evaluated as 63.5 mm for TD32-294, in light of the measured $T_{max} = 0.5$ kN, $k = 45$ kPa, and $L = 0.7$ m, which also compares well with the measured y_t of 62.5 mm. As expected, the values of k used here are higher than 25~30 kPa (explained later) adopted for the overall interaction illustrated in Fig. 17b.

- The estimated T_{max} and M_{max} must be capped by those deduced for the ultimate state.³

Example calculations of M_{max}

The current tests were conducted by translational movement of the loading block that has a loading angle of 16.7°. The sliding depth increases with the movement. The pre-

Fig. 19. Maximum shear force versus maximum bending moment. Measured data for (a) $L_m = 200$ and 350 mm and (b) various L_m , $d = 32$ mm.



vious model pile tests (Poulos et al. 1995) were carried out by rotating a loading block (rotational loading) about a constant sliding depth for each test. The current tests were generally associated with an effective soil movement, y_0 , of 30~70 mm ($= w_f - 37$ (mm) in Table 3), similar to the movement of 37 mm ($R_L < 0.5$) or 60 mm ($R_L > 0.5$) enforced previously (Poulos et al. 1995). Nevertheless, Fig. 18 shows a 3~5 times difference in the magnitudes of the measured bending moment, M_{max} , between the current and the previous tests. This difference and (or) impact is investigated here from three aspects using eqs. [5] and [6].

TS tests, TD tests, and k

The measured curves of $M_{max} \sim w_f$ and $T_{max} \sim w_f$ (see Figs. 13 and 17) were simulated regarding the pre-specified final sliding depths of 200 mm (TS tests) and 350 mm (TD tests), respectively. Elastic theory offers (Guo 2008a) $k/G_s = 2.841$ ($d = 50$ mm) and 2.516 ($d = 32$ mm). The G_s was de-

duced previously as 15~21 kPa, thus the k was obtained as 45~60 kPa ($d = 50$ mm). Given $w_i = 30$ mm (TD50-294) and 37 mm (TS50-294), the moment is thus calculated using $M_{max} = (w_f - w_i)kL^2/11.2$. They agree well with the measured data shown in the figures. As the diameter is changed to 32 mm, the k reduces to 25~35 kPa, in view of its proportional reduction to the diameter (resulting in 28.8~38.4 kPa), and further to the ratio of 2.516/2.841. This reduced k offers good estimations for the $d = 32$ mm tests as well, as shown in the figures. Equations [4]–[6] are thus sufficiently accurate for the deep and shallow sliding cases.

Translational loading with variable sliding depths (constant L)

The measured M_{max} of the piles TD32-0 and T32-0 ($L_m = 350$, Table 1) tested to a final sliding depth of 350 mm is presented in Table 3. It is modeled using $M_{max} = (w_f - 0.037)kL^2/11.2$ and $k = 35$ kPa. The estimated M_{max} for a series of w_f (or R_L) are also provided in Table 3 and plotted in Fig. 18a. The R_L was based on actual observation during the tests, which may be slightly different from the calculated one using $R_L = 0.33w_f/L$. The same calculation is also plotted in Fig. 18b. The moment increase at $R_L = 0.5$ (for $w_f > 120$ mm) was especially estimated using an additional movement of 30 mm beyond the w_f of 120 mm to show the (capped) ultimate value.³ Table 3 shows that the calculated value agrees with the two sets of measured M_{max} , in view of using the same w_i of 37 mm for either test.

Rotational loading about a fixed sliding depth

The M_{max} was obtained in model pile tests by loading with rotation about a fixed sliding depth (thus, a typical R_L) (Poulos et al. 1995). The results for a series of R_L were depicted in Fig. 18b and are tabulated in Table 4. This measured M_{max} is simulated via the following steps:

- The ratio of k/G_s was obtained as 2.39~2.79 using the closed-form expression by Guo and Lee (2001), which itself is a function of a factor γ ($= 1.05d/L$).
- Shear modulus was stipulated as $G_s = 10z$ (G_s in kPa, $z = L_s + L_m$ in m), from which the k was thus calculated.
- With $w_i = 0$ (as observed), the T_{max} was estimated using eq. [5] for $w_f = 37$ mm ($R_L < 0.5$) or $w_f = 60$ mm ($R_L > 0.5$).
- The M_{max} was calculated as $M_{max} = w_f k L^2 / 10$ as per eq. [6].

The test piles were of lengths 375~675 mm, and the G_s was 3.75~6.75 kPa. The values of the M_{max} calculated for the 10 model piles are provided in Table 4. They are plotted against the ratio R_L in Fig. 18b, which serves well as an upper bound of all the measured data.

Overall, eqs. [5] and [6] offer good estimations of M_{max} (thus, T_{max}) for all the current 12 model piles (e.g., Table 3) and the previous 10 tests (e.g., Table 4). The 3~5 times difference in the M_{max} is likely owing to the dominant impact of the pile dimensions (via L and the ratio k/G_s), the sub-grade modulus k , the effective movement ($w_f - w_i$), and the loading manner (w_i).

Calibration against in situ test piles

The simple correlations proposed here are validated using

Table 3. Calculation for translating pile test TD32-0 and T32-0 ($L_m = 350$ mm).

Input data			Calculated ^a		Measured M_{\max} (kN·mm)	
w_f (mm)	G_s (kPa)	R_L	T_{\max} (kN)	M_{\max} (kN·mm)	T32-0	TD32-0
30	14	0.1270	0	0	0.86	3.66
40	14	0.1693	0.018	4.62	2.78	8.80
50	14	0.2116	0.080	20.04	11.68	26.37
60	14	0.2540	0.142	35.45	21.69	44.42
70	14	0.2963	0.203	50.86	38.47	56.56
80	14	0.3386	0.265	66.27	63.96	57.50
90	14	0.3809	0.327	81.68	84.23	68.40
100	14	0.4233	0.388	97.09	97.51	85.17
110	14	0.4656	0.450	112.50	106.98	96.56
120	14	0.6398	0.512	127.92	118.12	119.50
150 ^b	14	0.7997	0.697	174.15	139.78	—

^a $w_i = 37$ mm, load transfer factor $\gamma = 0.048$, $k/G_s = 2.516$, $L = 0.7$ m, $d = 32$ mm.

^bTrapezoidal movement profile.

Table 4. Calculation for rotating tests (Poulos et al. 1995).

Input data				Calculated				Measured	
Embedded length L (mm)	w_f (mm)	G_s (kPa)	R_L	Factor γ (= $1.05d/L$)	k/G_s	T_{\max} (kN)	M_{\max} (kN·mm)	M_{\max} (kN·mm)	M_{\max} (kN·mm)
525	37	5.25	0.38	0.05000	2.54	0.0648	13.62	8.0	8.0
575	37	5.75	0.43	0.04565	2.48	0.0760	17.47	17.4	17.4
625	37	6.25	0.48	0.04200	2.43	0.0879	21.97	25.0	25.0
675	60	6.75	0.52	0.03889	2.39	0.1631	44.03	44.2	44.2
625	60	6.25	0.56	0.04200	2.43	0.1425	35.63	36.1	36.1
575	60	5.75	0.61	0.04565	2.48	0.1232	28.33	25.5	25.5
525	60	5.25	0.67	0.05000	2.54	0.1051	22.08	15.8	15.8
475	60	4.75	0.74	0.05526	2.61	0.0884	16.79	7.1	7.1
425	60	4.25	0.82	0.06176	2.69	0.0729	12.39	3.0	3.0
375	60	3.75	0.93	0.07000	2.79	0.0588	8.82	0.8	0.8

the measured response of eight in situ test piles and one centrifuge test pile subjected to soil movement. The pile and soil properties are tabulated in Table 5, along with the measured values of the maximum bending moment M_{\max} . The shear force, T_{\max} , however, was measured for three of the nine piles. The T_{\max} for the remaining six piles was thus taken as that deduced using elastic and elastic-plastic theory (Cai and Ugai 2003; see footnote 2 (footnote 1 in Web version)). The modulus of the subgrade reaction, k_i , and the equivalent length of the rigid pile, L_{ci} , were calculated previously.² The length L for each pile was taken as the smallest values of L_i and L_{ci} . This allows the ratio $M_{\max}/(T_{\max}L)$ for each case to be evaluated. The results are tabulated in Table 5 and are plotted in Fig. 20. The ratios all fall into the range of the elastic solutions based on a constant k for the plastic solution of eq. [3]. The slightly higher ratio for the exceptional Katamachi-B is anticipated.² It may be argued that four piles with a ratio of 0.26–0.4 exhibit elastic-plastic pile-soil interaction, with an eccentricity greater than zero.

Figure 19 shows that the ratio $M_{\max}/(T_{\max}L)$ from model pile tests stays almost invariably at 0.357 from the initial to ultimate loading state. The same ratio for the in situ pile (Frank and Pouget 2008) was calculated for the sliding and stable layers, respectively, with respect to the “pre-pull

back” (behaving as free head) and “after pull back” (fixed head) situation for the 16 years’ test duration. This ratio is plotted in Fig. 21. The ratio for the pile in the sliding layer stays around 0.25. (Note that the ratio for the stable layer as plotted in Fig. 21 seems to be complicated, but it is beyond the scope of this paper.) In brief, the ratio $M_{\max}/(T_{\max}L)$ is independent of loading level for either the model tests or the field test.

Determination of the T_{\max} is, however, more pertinent to pile head or base constraints. A fully fixed head observes $y_t = T_{\max}/(kL)$ (Guo and Lee 2001) and a semi-fixed head follows $y_t = (1 \sim 4)T_{\max}/(kL)$.

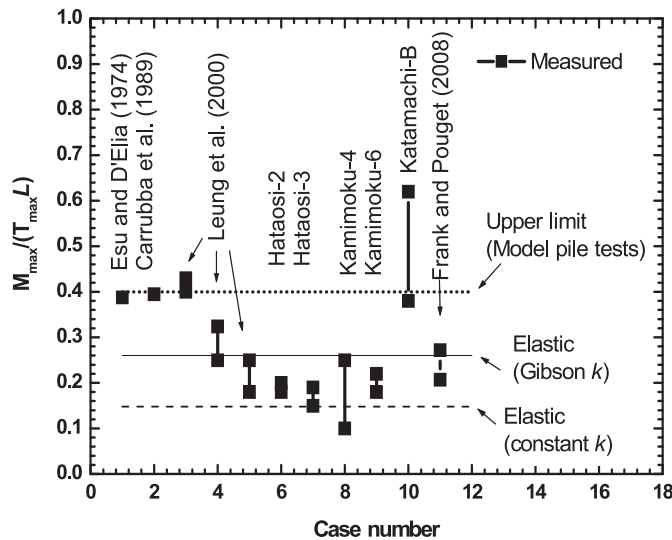
- The in situ pile (Frank and Pouget 2008) for the pre-pull back situation is evaluated using the free head solution. The k was obtained as 8.8 MPa (= $100s_u$, where undrained shear strength $s_u = 88$ kPa). At a groundline deflection $y_t = 32$ mm (recorded on 5 July 1995), the T_{\max} was estimated as 478.7 kN (= $y_t kL/4$). This T_{\max} agrees well with the measured load of 487 kN. Note that the measured pile deflection increases approximately linearly from groundline to a depth of 6.8–8.0 m, exhibiting “rigid” characteristics.
- The calculation of deflection and bending moment for rigid piles is illustrated in light of the two-row piles used to stabilize a sliding slope (Kalteziotis et al. 1993). Each

Table 5. $M_{max}/(T_{max}L)$ determined for field tests.

Piles			Soil		Measured			References
D/t^a (mm)	E_p^a (GPa)	L_1/L_2^a (m)	k_1/k_2^a (MPa)	L_{c1}/L_{c2}^a (m)	$M_{max}^{a,b}$ (kNm)	T_{max}^a (kN)	$M_{max}/(T_{max}L)^b$	
790/395	20	7.5/22.5	8.0/8.0	19.5/19.5	903	310	0.388	Esu and D'Elia (1974)
1200/600	20	9.5/13.0	15/15	12.7/12.7	2250	600	0.395	Carrubba et al. (1989)
630/315	28.45	2.5/10.0	14.4/28.8	23.1/23.1	60.2	56–60 ^c	0.40–0.43	Leung et al. (2000) (2.5 m)
630/315	28.45	3.5/9.0	14.4/28.8	23.1/23.1	73.8	65–85 ^c	0.25–0.32	Leung et al. (2000) (3.5 m)
630/315	28.45	4.5/8.0	14.4/28.8	23.1/23.1	81.2	72–100 ^c	0.18–0.25	Leung et al. (2000) (4.5 m)
318.5/6.9	210	11.2/12.8	5.0/8.0	6.3/5.6	165.2	144–150 ^c	0.18–0.20	Hataori-2 ^d
318.5/6.9	210	8.0/9.0	5.0/15.0	6.3/4.9	65.7	70–71.2 ^c	0.15–0.19	Hataori-3 ^d
318.5/6.9	210	6.5/7.5	5.0/8.0	6.3/5.6	197.2	143–300 ^c	0.10–0.25	Kamimoku-4 ^d
318.5/6.9	210	4.0/6.0	5.0/8.0	6.3/5.6	290.3	231–250 ^c	0.18–0.22	Kamimoku-6 ^d
300/60	20	7.3/5.7	6.0/10.0	3.2/2.8	69.5	40–56.2 ^c	0.38–0.62	Katamachi-B ^d
915/19	31.1 ^e	6.8/4.2	8.8/8.8	9.7/9.7	901.9 ^f	532.6 ^f	0.249 ^f	5 November 1986 ^g
					312.5 ^f	221.9 ^f	0.207 ^f	4 November 1986 ^g
					1102.3 ^f	642.3 ^f	0.252 ^f	11 November 1988 ^g
					536.6 ^f	369.5 ^f	0.214 ^f	10 November 1988 ^g
					1473.5 ^f	796.4 ^f	0.272 ^f	1 October 1992 ^g
					544.3 ^f	378.5 ^f	0.211 ^f	30 September 1992 ^g
					1434.2 ^f	834.7 ^f	0.253 ^f	6 July 1995 ^g
					756.1 ^f	487.0 ^f	0.228 ^f	5 July 1995 ^g

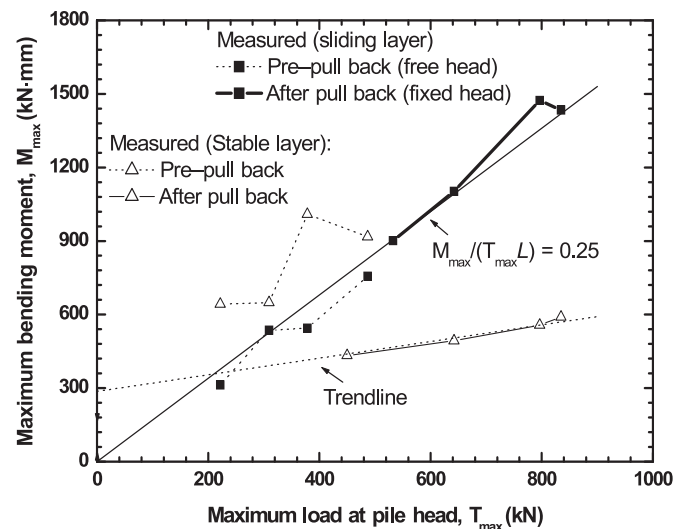
^aSee footnote 2 (footnote 1 in Web version); D , outside diameter; t , wall thickness; E_p , Young's modulus of pile; L_1/L_2 , thickness of sliding/stable layer; k_1/k_2 , subgrade modulus of sliding/stable layer; L_{c1}/L_{c2} , equivalent length for rigid pile in sliding/stable layer. In the estimation, G_{si} was simply taken as $k_i/3$.
^b M_{max} is the measured maximum bending moment; L is the the smallest value of L_i and L_{ci} .
^cEstimated using elastic and elastic-plastic solutions versus measured bending moment and pile deflection and soil movement profiles.
^dCai and Ugai (2003).
^eFlexural stiffness $E_p I_p = 1070 \text{ MN}\cdot\text{m}^2$.
^fAll for sliding layer.
^gFrank and Pouget (2008). Date shown refers to date that indicated values were recorded.

Fig. 20. Calculated versus measured ratios of $M_{max}/(T_{max}L)$.



steel pile had a length of 12 m, an external diameter of 1.03 m, a wall thickness, t , of 18 mm, and a flexural stiffness, $E_p I_p$, of 1540 MN·m². Given $k = k_1 = 15 \text{ MPa}$ (Chen and Poulos 1997) and an equivalent rigid pile length $L = L_1 = 4 \text{ m}$ (sliding depth), it follows that $T_{max} = 45 \text{ kN}$ ($= y_i k L / 4$) at $y_i = 0.003 \text{ m}$. This T_{max} compares well with the measured 40~45 kN. The T_{max} gives a uniform on-pile force per unit length of 10–11.25 kN/m. The moment is thus estimated as 80~90 kN·m

Fig. 21. Measured M_{max} and T_{max} (data from Frank and Pouget 2008).



($= 0.5 \times (10 \sim 11.25) \times 4^2$) about the sliding depth and as 180~202.5 kN·m about the 6 m depth. The average moment agrees well with the measured 150 kN·m, considering that the depth of sliding may be 4–6 m (Chow 1996; Chen and Poulos 1997).

Conclusions

An experimental apparatus was developed to investigate

the behaviour of vertically loaded, free head piles in sand undergoing lateral soil movement. A large number of tests have been conducted to date. Presented here are 14 typical tests concerning two diameters (32 and 50 mm), two loading levels (0 and 294 N, 7%–9% of the driving force), and varying sliding depths imposed by a triangular loading block. Results are provided for the applied force, induced shear force, bending moment, and deflection along the piles. The tests enable simple solutions to be proposed for predicting the pile response.

The model tests show the following features:

- M_{\max} is generally linearly related to the sliding force, T_{\max} , even for the initial frame movement up to w_i and the extra large w_f for the trapezoidal movement profile.
- Maximum bending moment increases by 60% for the 32 mm diameter piles or 30% for the 50 mm piles, and its depth increases by $\sim 50\%$, upon applying a static load of 7%–9% of the maximum driving force.
- 3–5 times different bending moments can occur given a similar size of model piles, but with a different loading manner.

With respect to the solutions, the following can be drawn:

- Equation [6] may be used to estimate the maximum bending moment, M_{\max} , for which the sliding thrust, T_{\max} , is calculated using eq. [5]. The estimation should adopt an effective frame movement of $w_f - w_i$, in which the w_i depends on the pile diameter, pile position, and loading manner.
- The subgrade modulus, k , may be estimated using the theoretical ratio of k/G_s and the shear modulus, G_s (e.g., 15–21 kPa in the current tests). The G_s is pertinent to either the overall shear process of the pile–soil–shear box system or the local pile–soil interaction. The k varies with diameter and should be considered accordingly.
- Based on the equivalent elastic pile–soil interaction, the T_{\max} from eq. [5] must be capped by the ultimate plastic state.

The current simple solutions, although approximate, offer satisfactory estimations of the 3–5 times different M_{\max} recorded in the current and previous model pile tests, and the correct ranges of $M_{\max}/(T_{\max}L)$ for eight in situ test piles and a centrifuge test pile.

Acknowledgements

The work reported here was supported by Australian Research Council Discovery Grant (DP0209027). The financial assistance is gratefully acknowledged. The authors would like to thank Mr. Enghow Ghee for his assistance with the experiment.

References

- Abdoun, T., Dobry, R., O'Rourke, T.D., and Goh, S.H. 2003. Pile response to lateral spreads: Centrifuge modeling. *Journal of Geotechnical and Geoenvironmental Engineering*, ASCE, **129**(10): 869–878. doi:10.1061/(ASCE)1090-0241(2003)129:10(869).
- Anagnostopoulos, C., and Georgiadis, M. 1993. Interaction of axial and lateral pile responses. *Journal of the Geotechnical Engineering Division*, ASCE, **119**(4): 793–798. doi:10.1061/(ASCE)0733-9410(1993)119:4(793).
- Aubeny, C.P., Han, S.W., and Murff, J.D. 2003. Inclined load capacity of suction caissons. *International Journal for Numerical and Analytical Methods in Geomechanics*, **27**(14): 1235–1254. doi:10.1002/nag.319.
- Bransby, M.F., and Springman, S.M. 1997. Centrifuge modelling of pile groups adjacent to surcharge loads. *Soils and Foundations*, **37**(2): 39–49.
- Broms, B. 1964. Lateral resistance of piles in cohesionless soils. *Journal of the Soil Mechanics and Foundation Engineering Division*, ASCE, **90**(3): 123–156.
- Cai, F., and Ugai, K. 2003. Response of flexible piles under laterally linear movement of the sliding layer in landslides. *Canadian Geotechnical Journal*, **40**(1): 46–53. doi:10.1139/t02-103.
- Carrubba, P., Maugeri, M., and Motta, E. 1989. Esperienze in vera grandezza sul comportamento di pali per la stabilizzazione di un pendio. *In Proceedings of the XVII Convegno Nazionale di Geotecnica*, Taormina, Italy, 26–28 April 1989. Associazione Geotecnica Italiana, Rome. Vol. 1, pp. 81–90. [In Italian.]
- Chen, L.T., and Poulos, H.G. 1997. Piles subjected to lateral soil movements. *Journal of Geotechnical and Geoenvironmental Engineering*, ASCE, **123**(9): 802–811. doi:10.1061/(ASCE)1090-0241(1997)123:9(802).
- Chmoulian, A. 2004. Briefing: Analysis of piled stabilisation of landslides. *Proceedings of the Institution of Civil Engineers*, *Geotechnical Engineering*, **157**(2): 55–56. doi:10.1680/geng.157.2.55.42388.
- Chow, Y.K. 1996. Analysis of piles used for slope stabilization. *International Journal for Numerical and Analytical Methods in Geomechanics*, **20**(9): 635–646. doi:10.1002/(SICI)1096-9853(199609)20:9<635::AID-NAG839>3.0.CO;2-X.
- Esu, F., and D'Elia, B. 1974. Interazione terreno-struttura in un palo sollecitato da una frana tipo colata. *Rivista Italiana di Geotecnica*, **8**(1): 27–38. [In Italian.]
- Frank, R., and Pouget, P. 2008. Experimental pile subjected to long duration thrusts owing to a moving slope. *Géotechnique*, **58**(8): 645–658. doi:10.1680/geot.2008.58.8.645.
- Fukuoka, M. 1977. The effects of horizontal loads on piles due to landslides. *In Proceedings of the 9th International Conference on Soil Mechanics and Foundation Engineering*, Specialty Session 10, Tokyo, 10–15 July 1977. Japanese Geotechnical Society, Tokyo. Vol. 1, pp. 27–42.
- Guo, W.D. 2003. A simplified approach for piles due to soil movement. *In Proceedings of the 12th Panamerican Conference on Soil Mechanics and Geotechnical Engineering*, Cambridge, Mass., 22–26 June 2003. Verlag Gluckauf GMBH, Essen, Germany. Vol. 2, pp. 2215–2220.
- Guo, W.D. 2008. Laterally loaded rigid piles in cohesionless soil. *Canadian Geotechnical Journal*, **45**(5): 676–697. doi:10.1139/T07-110.
- Guo, W.D., and Ghee, E.H. 2004. Model tests on single piles in sand subjected to lateral soil movement. *In Proceedings of the 18th Australasian Conference on the Mechanics of Structures and Materials*, Perth, Australia, 1–3 December 2004. Edited by A.J. Deeks and H. Hao A.A. Balkema, Rotterdam, the Netherlands. Vol. 2, pp. 997–1003.
- Guo, W.D., and Ghee, E.H. 2005. A preliminary investigation into the effect of axial load on piles subjected to lateral soil movement. *In Proceedings of the 1st International Symposium on Frontiers in Offshore Geotechnics*, Perth, Australia, 19–21 September 2005. Edited by S. Gourvenec and M. Cassidy. Taylor and Francis, London. Vol. 1, pp. 865–871.
- Guo, W.D., and Lee, F.H. 2001. Load transfer approach for laterally loaded piles. *International Journal for Numerical and Analy-*

- tical Methods in Geomechanics, **25**(11): 1101–1129. doi:10.1002/nag.169.
- Guo, W.D., and Qin, H.Y. 2006. Vertically loaded piles in sand subjected to triangular profiles of soil movements. *In* Proceedings of the 10th International Conference on Piling and Deep Foundations, Amsterdam, the Netherlands, 31 May – 2 June 2006. Deep Foundations Institute, Hawthorne, N.J. Vol. 1, Paper No. 1371.
- Guo, W.D., Qin, H.Y., and Ghee, E.H. 2006. Effect of soil movement profiles on vertically loaded single piles. *In* Proceedings of the 6th International Conference on Physical Modelling in Geotechnics, Hong Kong, 4–6 August 2006. Taylor and Francis Group plc, London. Vol. 2, pp. 841–846.
- Ito, T., and Matsui, T. 1975. Methods to estimate lateral force acting on stabilizing piles. *Soils and Foundations*, **15**(4): 43–59.
- Kalteziotis, N., Zervogiannis, H., Frank, R., Seve, G., and Berche, J.-C. 1993. Experimental study of landslide stabilization by large diameter piles. *In* Proceedings of the International Symposium on Geotechnical Engineering of Hard Soils – Soft Rocks, Athens. A. A. Balkema, Rotterdam, the Netherlands. Vol. 2, pp. 1115–1124.
- Karthigeyan, S., Ramakrishna, V.V.G.S.T., and Rajagopal, K. 2007. Numerical investigation of the effect of vertical load on the lateral response of piles. *Journal of Geotechnical and Geoenvironmental Engineering*, **133**(5): 512–521. doi:10.1061/(ASCE)1090-0241(2007)133:5(512).
- Knappett, J.A., and Madabhushi, S.P.G. 2009. Influence of axial load on lateral pile response in liquefiable soils. Part II: numerical modelling. *Géotechnique*, **59**(7): 583–592. doi:10.1680/geot.8.010.3750.
- Leung, C.F., Chow, Y.K., and Shen, R.F. 2000. Behaviour of pile subject to excavation-induced soil movement. *Journal of Geotechnical and Geoenvironmental Engineering*, ASCE, **126**(11): 947–954. doi:10.1061/(ASCE)1090-0241(2000)126:11(947).
- Meyerhof, G.G., Mathur, S.K., and Valsangkar, A.J. 1981. Lateral resistance and deflection of rigid wall and piles in layered soils. *Canadian Geotechnical Journal*, **18**(2): 159–170. doi:10.1139/t81-021.
- Meyerhof, G.G., Yalcin, A.S., and Mathur, S.K. 1983. Ultimate pile capacity for eccentric inclined load. *Journal of the Geotechnical Engineering Division, ASCE*, **109**(3): 408–423. doi:10.1061/(ASCE)0733-9410(1983)109:3(408).
- Pan, J.L., Goh, A.T.C., Wong, K.S., and Teh, C.I. 2002. Ultimate soil pressure for piles subjected to lateral soil movements. *Journal of Geotechnical and Geoenvironmental Engineering*, ASCE, **128**(6): 530–535. doi:10.1061/(ASCE)1090-0241(2002)128:6(530).
- Poulos, H.G. 1995. Design of reinforcing piles to increase slope stability. *Canadian Geotechnical Journal*, **32**(5): 808–818. doi:10.1139/t95-078.
- Poulos, H.G., Chen, L.T., and Hull, T.S. 1995. Model tests on single piles subjected to lateral soil movement. *Soils and Foundations*, **35**(4): 85–92.
- Scott, R.F. 1981. *Foundation analysis*. Prentice Hall, Englewood Cliffs, N.J.
- Smethurst, J.A., and Powrie, W. 2007. Monitoring and analysis of the bending behaviour of discrete piles used to stabilise a railway embankment. *Géotechnique*, **57**(8): 663–677. doi:10.1680/geot.2007.57.8.663.
- Stewart, D.P., Jewell, R.J., and Randolph, M.F. 1994. Design of piled bridge abutment on soft clay for loading from lateral soil movements. *Géotechnique*, **44**(2): 277–296.
- Viggiani, C. 1981. Ultimate lateral load on piles used to stabilise landslide. *In* Proceedings of the 10th International Conference on Soil Mechanics and Foundation Engineering, Stockholm, Sweden, 15–19 June 1981. A.A. Balkema, Rotterdam, the Netherlands. Vol. 3, pp. 555–560.